SEMARAK ILMU PUBLISHING

Journal of Advanced Research in Fluid Mechanics and Thermal Sciences

Journal homepage:
https://semarakilmu.com.my/journals/index.php/fluid_mechanics_thermal_sciences/index
ISSN: 2289-7879

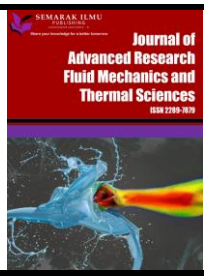

Thermal and Energy Influences of Double Skin Façade Towards Green Buildings in Tropical Classified Countries

Yonghuort Lim[1,2], Mohd Rodzi Ismail[1,*]

[1] School of Housing, Building and Planning, Universiti Sains Malaysia, 11800 USM, Penang, Malaysia
[2] General Department of Science, Technology and Innovation, Ministry of Industry, Science, Technology and Innovation, Cambodia

ARTICLE INFO

Article history:
Received 15 June 2023
Received in revised form 15 August 2023
Accepted 29 August 2023
Available online 17 September 2023

Keywords:
Double Skin Façade; Energy Efficiency; Built Environment; Simulation; Green Building; Tropical Climate

ABSTRACT

Double skin façade (DSF) has emerged as a decisive strategy for improving building thermal performance and energy efficiency. In various climatic conditions, DSF will perform differently and accordingly. However, the whole building performance of the DSF has never been studied in a broad climatic condition. As a result, there will be a high risk that the system will underperform conventional façade. This study adopted a quantitative approach with computational simulation software, EnergyPlus, to analyze the thermal behavior and energy efficiency of both single skin façade (SSF) and DSF systems. The investigation focused on an overall Köppen classified tropical climate category, which encompasses tropical rainforest (Af), tropical monsoon (Am), tropical savanna with dry winter (Aw), and tropical savanna with dry summer (As) climates. The primary finding indicates that the SSF in various tropical-classified groups exhibits diverse thermal behaviors throughout the year, from month to month and from orientation to orientation. The climate of each tropical classification distinctly influences the performance of both façades. The air temperature and relative humidity in both SSF and DSF office zones remained within a predictable range throughout the year. Thermal behavior and energy consumption fluctuated considerably on a monthly basis but only marginally on an annual basis. This similarity explains how buildings in the four cities consumed distinctly comparable cooling energy consumptions. The study also indicates that, even without a shading device, the DSF could still outperform the conventional facades. In all climatic contexts, energy consumption for cooling could be diminished by more than 40%, and the air temperature in the office zones was decreased to around 4°C while relative humidity was increased by 1% to 5%. Hence, an appropriate DSF design could be employed on office buildings in the overall classified tropical climates to attain energy efficiency through thermal enhancement from the façade's second layers.

1. Introduction

Double skin façade is one of the most appealing elements of a building's exterior due to its thermally responsive profits and aesthetically pleasing appearance [1]. Its applications are found in architectural and engineering design with frequently overlapping benefits [2]. The DSF has taken the

* *Corresponding author.*
E-mail address: rodzi@usm.my

https://doi.org/10.37934/arfmts.109.2.126

lead in architecture as an aesthetically environmentally friendly façade because it can satisfy glazing exterior desires, which in addition related to business trends while also positively responding to environmental issues [3,4]. For engineering, DSF is advantageous in terms of technical constructions and the physical environment. As Waldner *et al.,* [5] stated, DSF is formed by combining the traditional curtain walls and window system to ensure the wind and water tightness of the building, which was used in many engineering projects.

In today's design world, building envelopes, particularly glass façades, continue to play a significant role in fulfilling the functionality, desirability, and sustainability of a building. Additionally, designing envelopes to improve the energy performance of modern envelopes has been studied and explored for ages [6]. The application of DSF has become one of the key approaches to enhancing the performance of building envelopes contemplated by various findings [6,7]. The DSF has been widely known in temperate climates due to its significant impact on energy consumption and other indoor environmental benefits [4,8]. Similarly, its application has recently caught more attention in various climates due to its substantial influences and impacts on energy consumption and thermal performance in buildings, as demonstrated in different studies [1,9,10].

In a tropical climate, heat and glass facades are the most important influences on a building's energy performance. The glass façade retains a high solar radiation rate, heating the building and causing thermal discomfort as well as excessive energy consumption for air cooling systems. According to the United Nations Environment Programme, buildings consume more than 40% of global energy and roughly 60% of global electricity [11]. HVAC accounted for 56% of typical building total energy in tropical countries [12]. According to studies, the effects of DSF on building performance vary depending on location and climate [13-15]. Even though the DSF could effectively control heat gain caused by differences in indoor and outdoor temperatures as well as surface temperature, it could not prevent internal heat gain caused by direct solar radiation [16]. However, no comprehensive study has been conducted in a broad climate since it only focused on a single site. As a result, it could be the concern of simply adopting the system without broad knowledge in some locations or with proper DSF design. Nonetheless, there is a paucity of evidence demonstrating the benefit of DSF in terms of broader climatic conditions. Even though DSF technology has advanced in recent decades, problems persist when energy savings are not widely obtained, and its full capabilities have yet to be discovered [1]. Therefore, this study was carried out to evaluate the potential of DSF in an overall tropical classified climate by investigating its thermal behaviors and energy efficiency.

2. Double Skin Façade

2.1 Definition

Arons [17] defined the system as a twin skin façade made up of two divided planar walls that allow air to flow through them. Additionally, an immediate space allows ventilation to pass through while providing climatic and acoustic protection from the exterior layer. Like Boake *et al.,* [18], the air space between a pair of glass skins separated by an air corridor acts as insulation against extreme temperatures, winds, and noise. Sun-shading devices are frequently positioned between the two skins. All elements can be arranged in a variety of permutations and combinations of solid and transparent layers. Depending on the climatic location of the buildings, the distance of the intermediate air space can range from 20 centimeters to several meters to provide ventilation movement [7]. The ventilation of the cavity is regulated through a combination of fans, openings, and façade concepts. In cases where the ventilation is not controlled, various measures such as shading devices, motorized openings, or fans are often incorporated into the façade [2]. Another

similar explanation provided by Chan *et al.,* [19] defined a DSF as a building façade covering one or more stories with multiple glazed skins. The skins can be airtight or ventilated naturally or mechanically. Single glazing is typically used to harden the outer skin, but it can be fully glazed. In most applications, the inner skin can be insulated with double glazing but is not completely glazed.

Although definitions of the DSF differ in some ways, the system typically consists of two glass layers forming a cavity to deliver ventilation that can be operated naturally or mechanically depending on the context of the system's climate.

2.2 Classification

The classification of the DSF was made based on their characteristics and performances. Loncour *et al.,* [2] classified a DSF based on three main criteria: type of ventilation, façade partition, and cavity ventilation modes (Figure 1).

Partitioning describes how ventilation works between two glazing walls and how it is used in various situations. A ventilated double window, ventilated double façade per story with juxtaposed modules, corridor ventilated double façade per story, multi-storey ventilated double façade, multi-storey louver ventilated double façade and shaft-box ventilated double façade are the different types of the DSF cavity partitioning according to Loncour *et al.,* [2] as shown in Figure 1. Similarly, Poirazis [7] identified the four most commonly defined DSF systems based on geometry, which include box façade, corridor façade, shaft-box façade, and multi-storey façade.

Other methods of classifying the DSF are how air circulates in the cavity and how it is introduced into the cavity [20]. Figure 1 also indicates the five main classified characteristics of ventilation modes in the intermediate space of the DSF: indoor air curtain, outdoor air curtain, air supply, air exhaust and buffer zone.

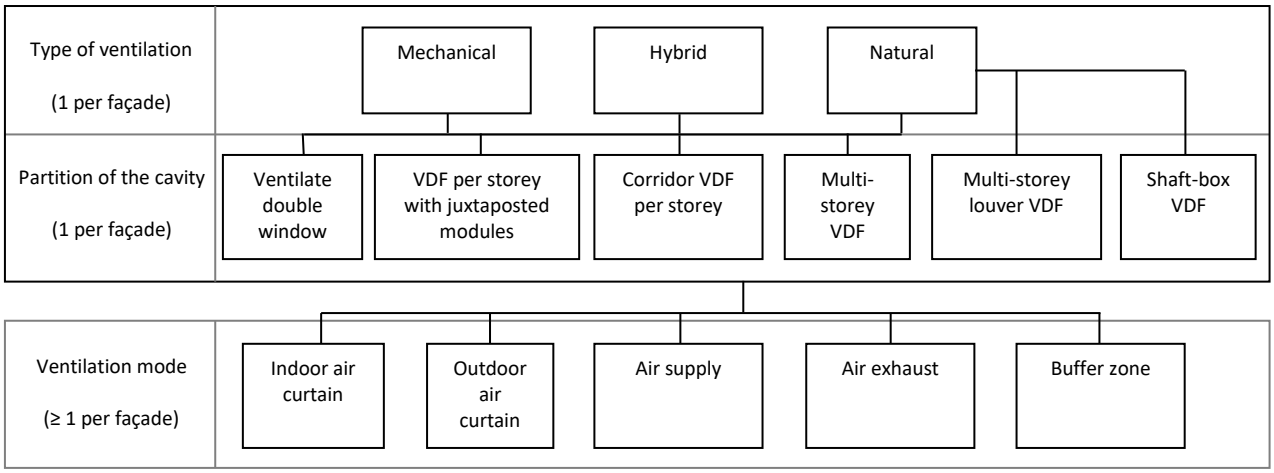

Fig. 1. DSF classification overview (VDF means DSF) [2]

2.3 Technical Aspects

There are numerous configuration aspects to consider in designing a proper DSF system. The three main components of a double façade are cavity depths, glass materials, and shading devices. These factors are crucial and can be designed in reverse to improve the DSF system's performance.

The DSF's intermediate space can range from centimeters to several meters, depending on how the designer wants it to perform. Aesthetic design, shading device variety, maintenance consideration, and ventilation mode play a role in determining the depth of the cavity [21]. The size

of the window opening influences the airflow characteristics of a naturally ventilated DSF [22]. On the other hand, the temperature in the DSF's intermediate space is significantly affected by opening size variation [23]. Regazzoli [24] demonstrated that the one-meter cavity depth of the multi-story DSF system is the most efficient, saving approximately 16% of building energy consumption compared to a conventional façade. Similarly, Rahmani *et al.,* [15] recommended one meter as the most effective depth for the DSF, even though the study was conducted on a fully air-conditioned office building in Malaysia's tropical climate. Furthermore, Aksamija [25] stated that a DSF with a one-meter air gap provided better results in terms of reducing cooling loads in the building.

According to a recent study by Tao *et al.,* [26], the proper glazing on the DSF façade improves ventilation significantly. The study was conducted on a naturally ventilated DSF and discovered that replacing the clear glazing with low-e glazing on the building's DSF façade could increase ventilation by 13%. On the other hand, the climatic context affects glazing selection [21]. According to Streicher *et al.,* [4], the DSF system typology largely determines the glazing types of the internal and external layers of the DSF. They also stated that when the system uses outdoor air for ventilation, single glazing is normally applied on the exterior skin while the insulating pane is on the interior. If the system uses indoor air, the materials are in the reverse direction. To achieve potential heat gain reduction, Haase and Amato [27] recommended using two clear glazing for the interior and exterior layers of the ventilated DSF. Aksamija [25] suggested that the double-glazing exterior could improve the overall performance of the facade and result in energy savings.

The DSF can improve building energy efficiency even without shading devices. However, the presence of shading devices in or on the DSF cavity could improve performance even further [28]. A recent study by Kim [23] found that shading devices could reduce the temperature in the cavity. Another study by Kim *et al.,* [29] found that using the center blind for ventilated DSF results in the highest annual total load reduction in the building while using the exterior blind results in the second highest. Lee *et al.,* [30] reported preliminary findings on the effects of shading device positions on air temperature and airflow patterns between the two layers of the DSF. One of the most important factors in estimating heat transfer through the DSF intermediate space is the placement of shading devices [31]. On the other hand, the device's properties may reduce the heating of the façades [32]. He also mentioned that the light color blind may allow a greater percentage of light into the room. Furthermore, energy performance in the DSF is said to be functional and efficient when shading devices are properly planned and controlled [33,34]. Determining the effective characteristics of the sun shading in each case poses a problem at the planning stage because the properties can vary significantly depending on the type of glazing and ventilation of the sun shading system [35].

2.4 Thermal Energy Performance

The primary heat transfer agent through the DSF exterior glazing layer is solar radiation. It passes directly through the glazing layer, with approximately 15% initial reflection depending on the outdoor environment, and the remaining radiation passes through the glass [36]. As the exterior skins are heated by solar radiation, the temperature in the cavity rises, pushing air circulation and creating a greenhouse effect [37]. Another factor influencing thermal transfer in the DSF is the so-called chimney or stack effect. The stack effect is a phenomenon related to the rising of hot air, which is lighter than cold air. When the air in the intermediate space becomes warmer than the air outside, it tends to discharge at the very top of the façade, increasing the airflow rate in the façade cavity [2]. From these behaviors, DSF could offer adaptability to both cooler and warmer weather conditions, making them highly intriguing. By making minor adjustments such as opening or closing inlet or outlet fins or activating air circulators, the behavior of the façade can be modified. In colder climates, the

air buffer within the DSF acts as a barrier against heat loss. The sun-heated air trapped in the cavity can be used to warm spaces outside the glass, reducing the need for indoor heating systems. However, in hot climates, the DSF can be vented outside the building to mitigate solar gain and decrease the cooling load. This is achieved through a process called the chimney effect, where differences in air density create a circular motion that allows excess heat to escape. As the air temperature within the cavity rises, it is pushed out, creating a slight breeze in the surroundings while effectively preventing heat gain, as shown in Figure 2 [38].

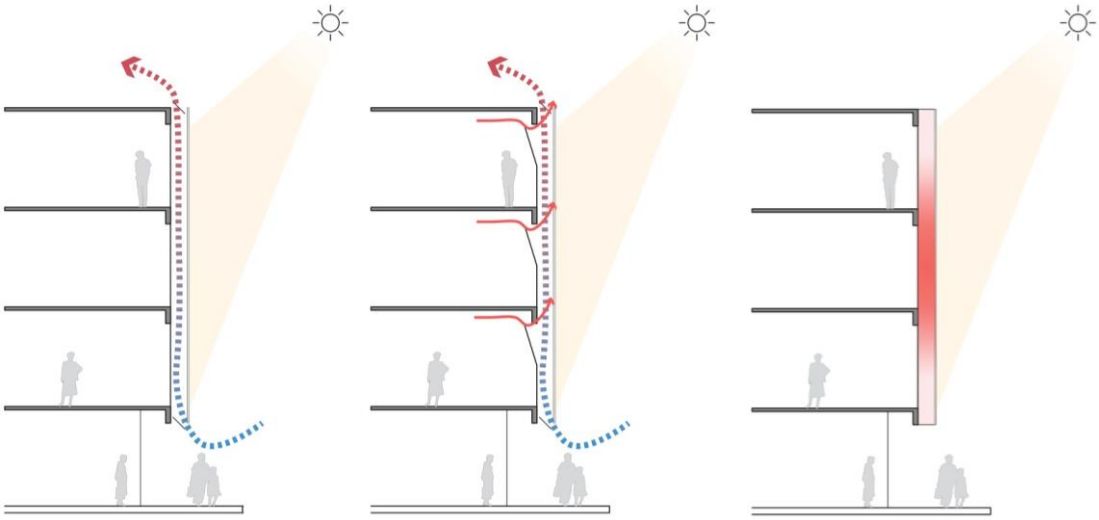

Fig. 2. Optimal ventilation and thermal control of the DSF system during both (a) summer and (b) winter seasons [38]

In different climatic contexts, structural configurations have a provocative effect on the thermal performances of the DSF [39]. Theoretically, the DSF could control heat gained from temperature differences between indoor and outdoor temperatures, as well as temperature differences on the glass surface [16]. However, the DSF is unable to block internal heat gain from direct solar radiation and requires proper design in order to avoid overheating, particularly during the hot season [16,40]. The glazing extent of the DSF is directly related to the heating and cooling energy consumption because it is the primary component influencing heat losses and heat gains through the glass surfaces [41]. The DSF could improve the building's energy efficiency due to lower transmission losses and how the cavity air is used. To precisely assess the energy efficiency of the DSF, it is necessary to investigate not only the transmission gains and losses but also the enthalpy change of the cavity air and conduct a whole-building energy analysis. However, most typologies cannot reduce both annual heating and cooling demand. Combining typologies or changing system settings based on the specific situation alone could provide a significant overall improvement over the conventional façade. This implies that sophisticated control mechanisms are required to ensure that DSF functions properly throughout the year with proper heating and cooling evaluation [20].

3. Methodology

A range of methods, both existing and newly developed, have been employed to assess the thermal and energy performance of buildings. These methods encompass statistical approaches as well as simulation-based techniques, providing comprehensive insights into the efficiency of buildings in terms of thermal and energy management [42]. Many simulations have been available

for whole-building simulation, such as BLAST, DOE 2, eQUEST, TRNSYS, EnergyPlus, Energy Express, EFEN, and so on [43]. In some presentations, online building energy predictions based on neural networks and genetic algorithms could also be used [44].

This research study adopted a quantitative research approach along with computational simulation software, EnergyPlus, to investigate the thermal performance and energy consumption of DSF buildings in an overall tropical climate, which was represented by the four countries having different tropical climate characteristics, as classified by Köppen [45]. These selected countries represented other tropical locations in the same group (Figure 3). Reflecting this purpose, a base case office building with typical characteristics was proposed for investigations.

The two data sets to be collected were weather data and the building's physical information of the office building from the selected cities. Weather data is typically obtained from the EnergyPlus database, which contains all the environmental parameters of a specific location, such as air temperature, relative humidity, air flow rate, and so on. However, weather data of the selected cities for this study were from the EnergyPlus database and annual observations from the respective weather forecast stations. The building's physical information of the proposed base case building was derived from desk reviews and the survey of various office buildings in the selected cities. Building construction, HVAC system, electrical equipment, and building occupancy were all included.

The three main environmental parameters consisting of air temperature, relative humidity and solar radiation were analyzed, and the total energy consumption of air-conditioning was obtained for benchmarking in each tropical category. Building orientations were also considered for thermal analyses. It is worth mentioning that in order to find the potential of the DSF alone, a shading device was not employed in the DSF model for this study.

3.1 Simulation Tool

3.1.1 EnergyPlus

EnergyPlus is an official simulation program of the United States Department of Energy, promoted through the Building and Technology Program of the Energy Efficiency and Renewable Energy Office. EnergyPlus is a widespread and accepted tool in the building energy analysis community around the world [46]. The roots of EnergyPlus were combined with BLAST (Building Loads Analysis and System Thermodynamics) and DOE-2, which are the computer programs for the design of energy-efficient buildings developed for the U.S. Department of Energy. Both programs were developed and released in the late 1970s and early 1980s as energy and load simulation tools intended for design architects and engineers. On the other hand, ASHRAE is the base reference for EnergyPlus calculation [47]. EnergyPlus is a console-based program that reads input and writes output to text files. It ships with several utilities, including IDF-Editor for creating input files using a simple spreadsheet-like interface, EP-Launch for managing input and output files and performing batch simulations, and EP-Compare for graphically comparing the results of two or more simulations. Several comprehensive graphical interfaces for EnergyPlus are also available [47]. For this research, EnergyPlus version 22.1.0 was used for assessing the whole building's thermal and energy performance, along with OpenStudio and Google SketchUp to model the building interface of the base case models.

3.1.2 Validation

It has been more than a decade since EnergyPlus has been validated and widely employed by numerous studies since the tool could provide many benefits in terms of time efficiency with reliable

simulating results. Table 1 indicates experimental validation studies that examine and demonstrate the reliability and effectiveness of the simulation tool, EnergyPlus, with various DSF classifications and climates over the years. There were studies on tool experimental validation following the International Performance Measurement and Verification Protocol 2012 [48-51]. Joe *et al.,* [48] and Anđelković *et al.,* [49] used similar approaches to conduct experimental validation on a multi-story ventilated DSF in humid subtropical climates. Mean Bias Error (MBE), Root Mean Square Error (RMSE) and coefficient of determination (R^2) were used for quantifying the deviation between the measurement and simulation. MBE is a statistical indicator that indicates the average deviation of values predicted in the model from actual (measured) values of the observed phenomenon, as shown in Eq. (1). A positive value of this indicator indicates that the model over-predicts values, whereas a negative value indicates that the model under-predicts the observed phenomenon's value. A low MBE value is desired. The RSME indicator is frequently used to assess the difference between simulation results and measurement values. The RMSE of a data series indicates how it differs from other data series. This indicator suggests the average mean deviation (error) and the degree of data variation but provides no explicit information on the relative magnitude of the average difference between the predicted and recorded values, as shown in Eq. (2). The ideal value of RMSE is zero and always positive. The determination coefficient represents the proportion of explained variance in total variance. As a measure of regression quality, it indicates how much of the variation in the dependent variable (simulation results) is explained by the model and how much is explained by variations in the independent variable (measurement results), demonstrated in Eq. (3). The study's findings show a high level of agreement and matching between measured and simulated values, confirming the dependability and effectiveness of the used energy simulation tool.

$$MBE = \frac{\sum_{i=1}^{n}(M_i - S_i)}{n} \tag{1}$$

$$RMSE = \sqrt{\frac{\sum_{i=1}^{n}(M_i - S_i)^2}{n}} \tag{2}$$

$$R^2 = \left(\frac{\left(n\sum_{i=1}^{n}(M_i S_i) - \left(\sum_{i=1}^{n} M_i\right)\left(\sum_{i=1}^{n} S_i\right)\right)^2}{\left(n\left(\sum_{i=1}^{n}({M_i}^2) - \sum_{i=1}^{n}({M_i}^2)\right)\right)\left(n\left(\sum_{i=1}^{n}({S_i}^2) - \sum_{i=1}^{n}({S_i}^2)\right)\right)} \right) \tag{3}$$

When the number of measurements and simulations is limited, Anđelković *et al.,* [49] replace n with n-1, which is the number of degrees of freedom. Degrees of freedom is derived from the geometric representation of the problem associated with RMSE; the calculations are formulated to Eq. (4) and Eq. (5). In addition, the coefficient of variation of the root means squared error (CV(RMSE)) was used in their experimental validation. The CV(RMSE) measures the relationship between the RMSE and the arithmetic mean, as indicated in Eq. (6). It is commonly expressed in percentages and denotes the proportion of RMSE in the arithmetic mean.

$$MBE = \frac{\sum_{i=1}^{n}(M_i - S_i)}{n-1} \tag{4}$$

$$RMSE = \sqrt{\frac{\sum_{i=1}^{n}(M_i - S_i)^2}{n-1}} \tag{5}$$

$$CV(RMSE) = \frac{RMSE}{N} * 100 \tag{6}$$

Similarly, Im *et al.,* [50] used a flexible research platform to conduct validation of EnergyPlus. The study provided reliable empirical data for ANSI/ASHRAE Standard 140, Standard Method of Test for the Evaluation of Building Energy Analysis Computer Programs, in order to improve the accuracy of building energy model (BEM) engines and better characterize their accuracy. Slightly apart from the above studies, Im *et al.,* [50] used Normalized Mean Bias Error (NMBE) for quantifying the deviation between the measurement and simulation; calculations are expressed in Eq. (7) and Eq. (8) while the arithmetic value/mean of measured data, N, is expressed in Eq. (9). Without any calibration efforts, the EnergyPlus model is built from as-built drawings and in-situ experimental data. The energy consumption from the simulation and experimental are well matched and hourly NMBE and CV(RMSE) for both Tests are quite small.

$$NMBE = \frac{1}{M} * \frac{\sum_{i=1}^{n}(M_i - S_i)}{n} * 100 \quad (7)$$

$$CV(RMSE) = \frac{1}{M} * \sqrt{\frac{\sum_{i=1}^{n}(M_i - S_i)^2}{n}} * 100 \quad (8)$$

$$N = \frac{\sum_{i=1}^{n}(M_i)}{n} \quad (9)$$

where:
N is arithmetic value/mean of measured data;
M_i is measured value at one point;
S_i is the value obtained by simulation;
n is the total number of measurements;
CV is the coefficient of variation

Table 1
Research studies that have employed and validated EnergyPlus for their analytical experiments

Research study	Location/ Climate	Validation approach/Key findings	Key references	Year
Investigation on the energy performance of double skin façade in Hong Kong	Hong Kong	Computer model/Experimental setup The computer simulation model accurately represents the real situation and is reliable for predicting the energy performance of the DSF in Hong Kong buildings.	Chan *et al.,* [19]	2009
Energy performance assessment of double-skin facade with thermal mass	Munich	Numerical model/Experimental data The model prediction and the measured data are in good agreement. A similar agreement was also observed in other studies.	Fallahi *et al.,* [52]	2010
Verification and validation of EnergyPlus phase change material model for opaque wall assemblies	-	Analytical verification/Comparative testing/Empirical validation As two bugs in the PCM model were identified and fixed, the PCM model in EnergyPlus was verified and validated.	Tabares-Velasco *et al.,* [53]	2012
Sensitivity analysis and validation of an EnergyPlus model of a house in Upper Austria	Hagenberg, Austria	Calculation/Measurement/Simulation Using more precise weather data can improve the fit of simulations to real-world	Pereira *et al.,* [54]	2014

		measurements. The predictions of direct solar radiation for the EnergyPlus weather file can already improve the fits of the indoor simulation temperature and reduce the mean absolute error (MAE).		
Load characteristics and operation strategies of building integrated with multi-story double skin facade	Seoul, Korea	Measurement/Simulation Validation indicates that the error range is generally reliable.	Joe *et al.,* [48]	2014
Validation of EnergyPlus thermal simulation of a double skin naturally and mechanically ventilated test cell	Lisbon, Portuguese	Empirical validation with measurement data/Experiment Simulation and experiment agree well, with an average simulation error in air and radiant temperature of 1.4^{o}C and an average daily maximum error of 2.5^{o}C.	Mateus *et al.,* [55]	2014
Experimental validation of EnergyPlus model: Application of a multi-storey naturally ventilated double skin façade	Belgrade, Serbia	Numerical simulation/Measurement There is a high level of agreement and matching between measured values and simulated results, confirming the effectiveness of the employed energy simulation tool.	Anđelković *et al.,* [49]	2016
Empirical validation of building energy modeling using Flexible Research Platform	Oak Ridge, Tennessee, USA	Empirical validation/Experimental data The RTU's simulation and experimental energy consumption are well matched. For both Tests, the hourly NMBE and CV(RMSE) are less than 2.5% and 5.8%, respectively.	Im *et al.,* [50]	2019
Modeling double skin façades (DSFs) in whole-building energy simulation tools: Validation and inter-software comparison of a mechanically ventilated single-story DSF	Northern Italy	Numerical simulations/Experimental data No tool is outstandingly better performing over the others, but some tools offer better predictions when the focus is placed on certain thermophysical quantities, while others should be chosen if the focus is on different ones.	Lucchino *et al.,* [51]	2021

3.2 Weather Data

The weather data contains all the environmental parameters observed annually. The weather data used in EnergyPlus is a simple text-based format, similar to the input and output data files. Its format is EPW, which includes the basic site information consisting of location, data source, latitude, longitude, time zone, elevation, peak heating and cooling design conditions, holidays, daylight saving period, typical and extreme periods, two lines for comments, and period covered by the data. The EPW file format was developed for the EnergyPlus building simulation model of the U.S. Department of Energy [47].

The Köppen classification system categorizes global climate into five major types, denoted by capital letters: A (tropical), B (arid), C (temperate), D (cold), and E. (polar) [56]. Group A which represents the overall tropical climate has been chosen for this study. This classification has every month of the year with an average temperature of 18 °C (64.4 °F) or higher, with significant precipitation and its sub-classifications are itemized as follows (Figure 3).

(i) Af: Tropical rainforest climate; average precipitation of at least 60 mm (2.4 in) every month.
(ii) Am: Tropical monsoon climate; driest month (which nearly always occurs at or soon after the "winter" solstice for that side of the equator) with precipitation less than 60 mm (2.4 in), but at least 100-(Total Annual Precipitation (mm)/25).
(iii) Aw or As: Tropical wet and dry or savanna climate; with the driest month having precipitation less than 60 mm (2.4 in) and less than 100-(Total Annual Precipitation (mm)/25).

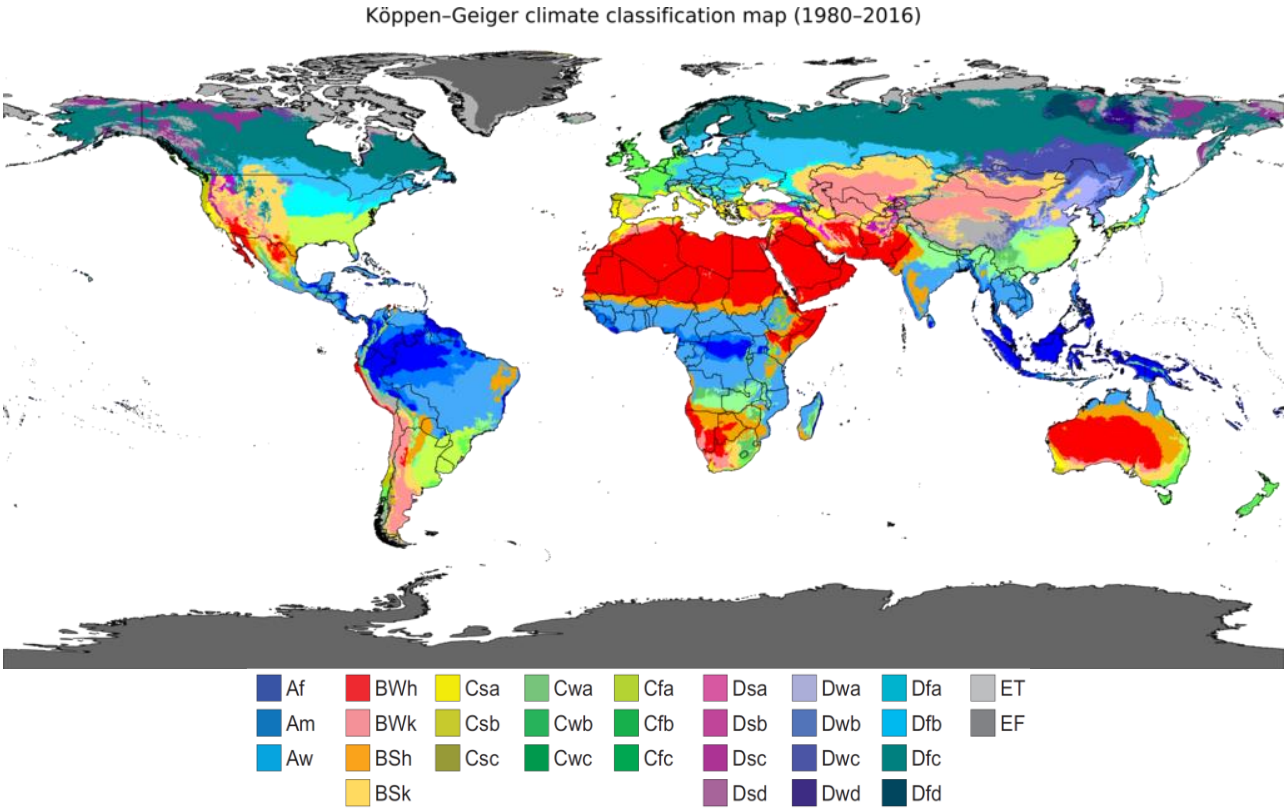

Fig. 3. Köppen tropical climate classification [56]

For this research, the weather files are a typical year file (TYP) obtained from the EnergyPlus database and annual observations from each city's weather forecast station. Even though the climates of the four cities are in the tropical group, their annual temperature is comparatively different. The comparison of average temperatures between the four tropical classified cities is shown in Figure 4. The four selected cities that represent the four tropical classifications are shown in Table 2.

Table 2
The selection of cities for various weather investigation

Group A	Characteristic	City	Country
Af	Tropical rainforest climate	Kuala Lumpur	Malaysia
Am	Tropical monsoon climate	Jakarta	Indonesia
Aw	Tropical savanna climate with dry winter	Phnom Penh	Cambodia
As	Tropical savanna climate with dry summer	Nha Trang	Vietnam

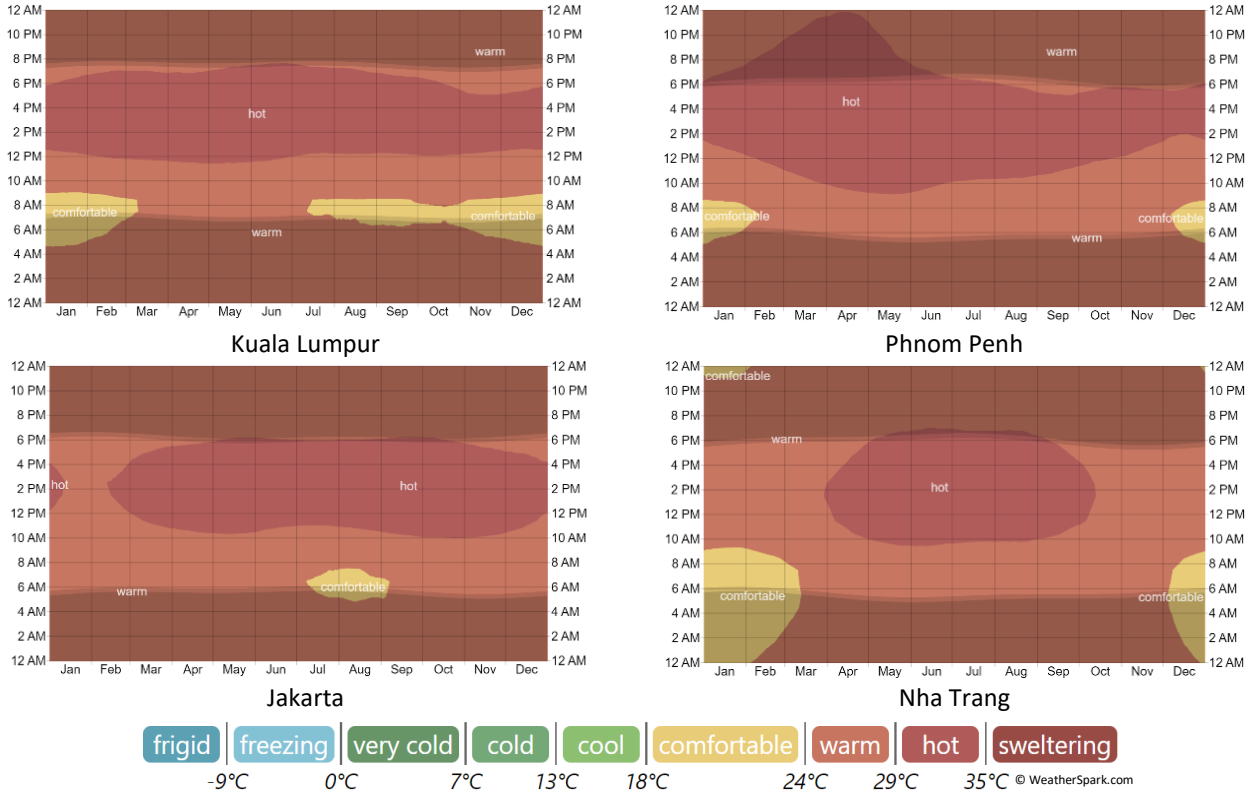

Fig. 4. The comparison of the average hourly temperature between the selected cities

3.3 Base Case Building

This section described and justified how the base case model was formulated for the analytical investigation. Mostly, the common material of the office building is glass walls or windows, along with the electrical equipment and HVAC system applied onto the structural components, which normally are concrete and steel. To investigate the performance of the DSF in a broad tropical climate, the base case model is proposed based on the office building characteristics in the selected locations (Table 2). Thus, the office buildings located in those classified climates are significantly studied. The building's physical information of the based case model was proposed based on the average basis and indicated in Table 3 below.

The DSF version of the base case building is designed following the optimal configurations for the specific tropical climate region recommended by various research findings. The list of recommendations from various research studies can be found in Lim *et al.,* [57]. The selected classification and the technical aspect of the DSF base case model are shown the Table 4. It is worth mentioning that, to investigate the potential of the double glass layer alone, a shading device was not proposed in the studied DSF model.

The whole building energy modeling of the base case building is shown in Figure 5(a), while Figure 5(b) illustrates the thermal zone and section of the base case building. The floor plan was divided into nine thermal zones, each with four office zones (SSF), four cavity zones (DSF), and a center core zone.

Table 3
The physical building's information of the based case model

Elements	Properties
Building type:	Office
Level:	20 stories
Ground floor area:	400sq.m
North length:	20m
South length:	20m
West width	20m
East width:	20m
Total height:	87.5m
Wall:	Double brick plaster
Roof ceiling:	100mm concrete and 10mm plasterboard
Floor:	100mm concrete slab
Glass type:	Double low-e glazing
Window shading:	Venetian blind
Lighting type:	Open fluorescent luminaire/ Recessed round downlight
Cooling type:	Air-cooled
HVAC:	VAV system
Operating schedule:	7:00 to 17:00
Working day:	Monday-Friday
Weather data:	Respective cities

Table 4
The optimal configurations selected for the DSF model

Classification	
Partition:	Multi-Storey
Ventilation Mode:	Outdoor Air Curtain
Ventilation Type:	Natural
Technical Aspect	
Cavity Depth:	1000mm
Exterior Glazing Materials:	Double Low-e Glazing
Shading Device:	None

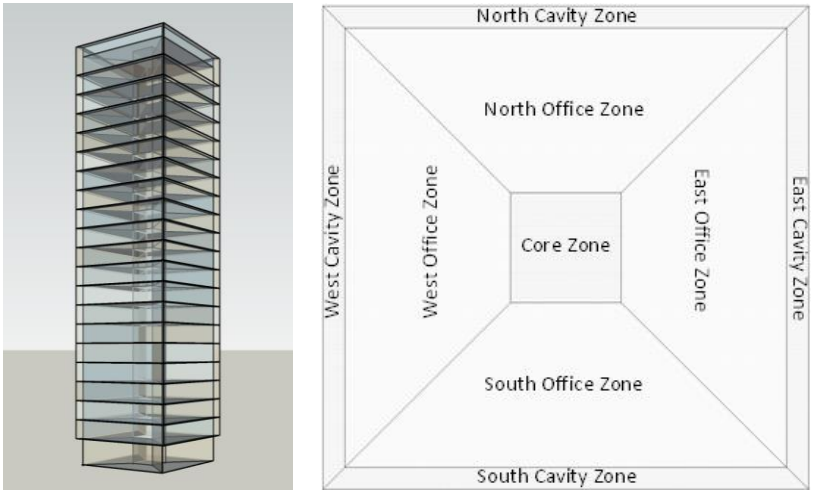

(a) (b)

Fig. 5. (a) Thermal zones of each floor (b) The whole building energy modeling of the base case model

4. Result Analysis

Both SSF and DSF models were designed to be the most efficient classification, comprising all the most efficient aspects, as recommended for tropical contexts [57]. The performances of both facades were investigated in the selected climate categories. The results of three main thermal parameters, including air temperature, relative humidity, and solar radiation, with the energy consumption of buildings, were all crucial for this comprehensive analysis. Each thermal parameter was thoroughly analyzed in sequence from the SSF to the DSF system to the comparisons of both façade categories.

4.1 Zone Air Temperature

When we first only look at the SSF, the air temperatures in the thermal office zones of the SSF in each city varied throughout the year. The temperature in Phnom Penh city was high from February to April, with the highest temperature of 51°C and gradually dropped from May to October, with the lowest of only 42°C, which was also the lowest among the cities. Kuala Lumpur had a nearly constant temperature throughout the year, ranging from 47°C to 50°C. Jakarta began with the lowest temperature of 45°C in January and gradually rose, reaching its highest peak in May, with more than 53°C, the highest of all. Nha Trang city had the lowest temperatures between November and December, with around 44°C and the peak temperatures between June and August, which could reach up to 53°C (Figure 6).

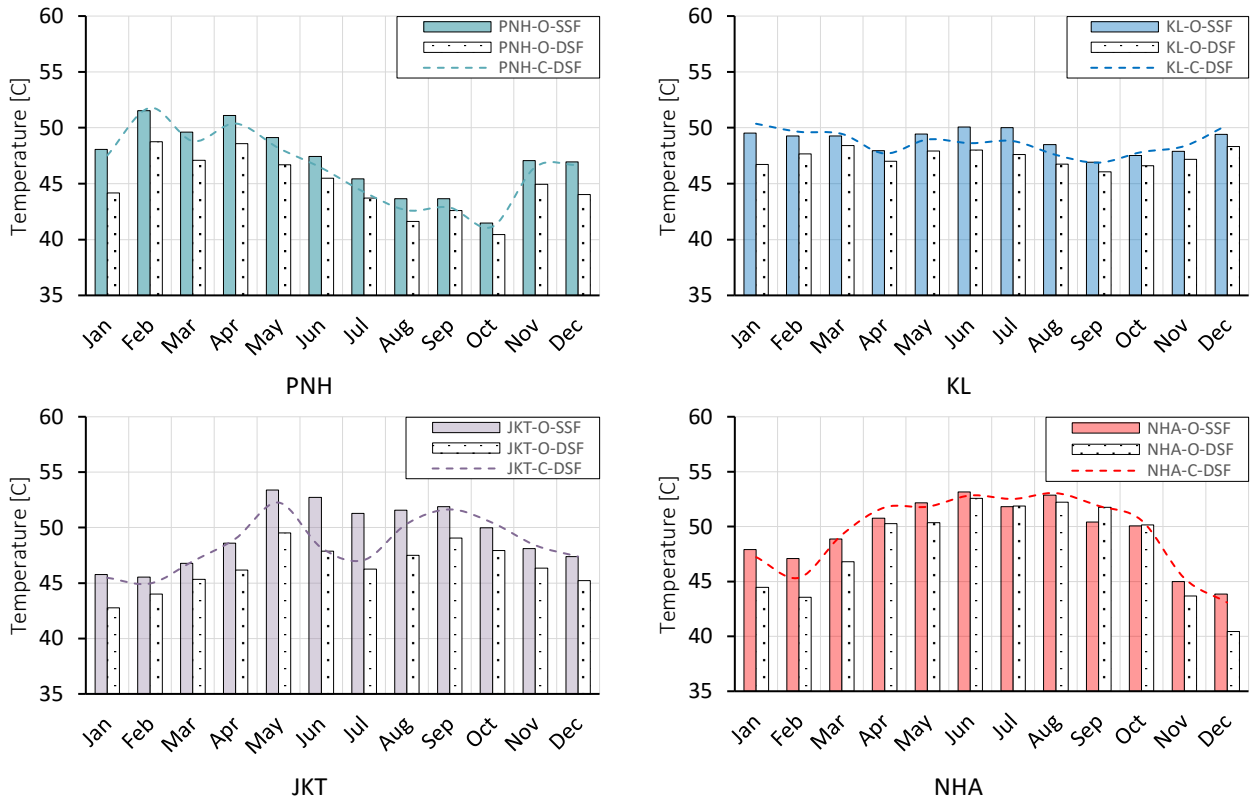

Fig. 6. Monthly average air temperature in the thermal zones of SSF and DSF of each city

From the temperature variations of the SSF façade above, the air temperatures in the thermal zones of the DSF in each city also varied all year. It was noticeable that all thermal office zones were likely cooler than the thermal cavity zone almost all year round. The fluctuations in temperatures were quite similar to the SSF on a monthly basis. On average, thermal office zones in the four cities

were cooler than thermal cavity zones by around 2°C. However, temperatures in thermal office zones in Nha Trang were somehow hotter than in the cavity zone (Figure 6).

Even though the air temperature of the office zones of SSF had remarkably dropped around 1°C to 3°C on an annual average compared to the respective office zones of DSF, air temperatures in the DSF cavity zone were somehow lower than in the SSF office zone. For instance, cavity zones in Phnom Penh and Jakarta city were generally lower than the SSF office zone around 1°C. Even so, that was not all the case for other cities, such as the DSF cavity zones of Kuala Lumpur were lower than the SSF office zones from April to September by around 1°C, while the rest were hotter, with also around 1°C. Even if the temperatures of the DSF office zones were typically lower than the ones in the SSF office zones, the DSF office zones were also equal to or slightly hotter than their cavity zones (Figure 7). As indicated in Figure 6, the temperatures of the cavity zones in Nha Trang were lower than their office zones in July. It could be explained by the thermal investigation in the following section on the thermal performance of the DSF at all orientations that the temperature in the DSF office zone could be somehow hotter than its cavity.

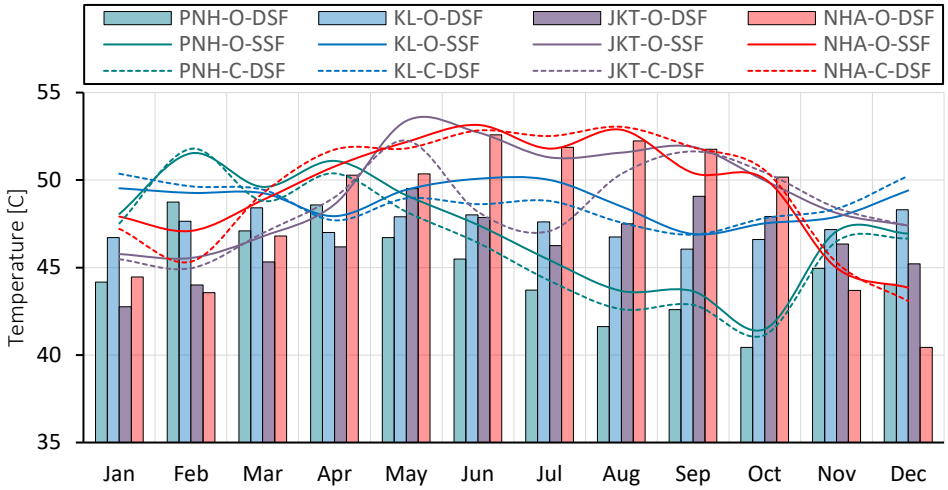

Fig. 7. Comparison of monthly average air temperature in the thermal zones of SSF and DSF of each city

Looking at the annual average air temperature in the thermal zones of SSF at the four orientations of each city, the SSF's annual hottest thermal zones of the four cities were the same in the east, with Kuala Lumpur being the highest of all. Nevertheless, the annual coolest orientations of each city differed, with Phnom Penh and Nha Trang in the north, Kuala Lumpur in the west, and Jakarta in the south. The air temperatures in each thermal office zone of the four cities changed from orientation to orientation on a monthly basis (Figure 8).

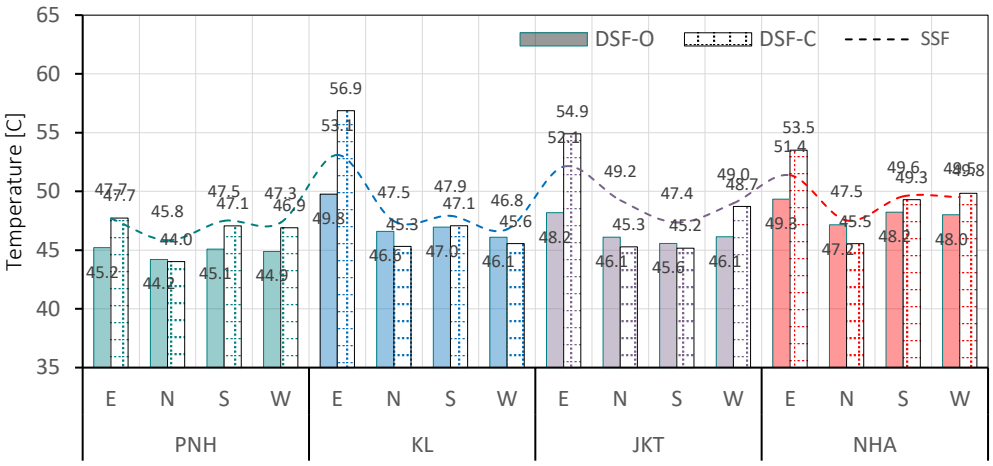

Fig. 8. Comparison of annual average air temperature in the thermal zones of SSF and DSF at the four orientations of each city

When comparing all thermal cavity zones of DSF with their respective office zones in all climatic categories, the temperatures in the cavity zones were normally higher than its office zones in all cases, except for all the north, where the cavity zones were cooler than its office zones by around 1°C to 2°C. Furthermore, there was a special case for Kuala Lumpur that both the north and the west office zones were hotter than their cavity. Despite this, the temperatures of the north office zones of all locations, including the west office zone in Kuala Lumpur, were still lower than all other zones having a hotter cavity. Otherwise, the air temperatures in every office zone having a cooler cavity were always the lowest among all orientations (Figure 8).

It can also be seen that air temperatures of the SSF office zones in all locations remarkably dropped around 1°C to 3°C. All orientations of the four climate classifications had a typical temperature range of only around 3°C. Interestingly, both the office zone and the cavity zone of the DSF were lower than the SSF office zone at all orientations in all cities, except for the east, where the cavity zones were hotter than the SSF office zones (Figure 8). These phenomena could also be explained by the extra layer of DSF that diminished solar radiation with the enhancement of the thermal stack effect inside the cavity, cooling down the interior zone and the behaviors of the respective locations, where the east seemed to have the highest temperature the entire year, which may significantly affect the chimney effect in the cavity of the DSF, increasing the temperature with a higher solar radiation rate annually.

4.2 Zone Air Relative Humidity

In the SSF system, relative humidity in the thermal office zone of Phnom Penh city was by far the lowest and highest among all; it reached its peak from August to October and its lowest point in February, with humidity levels ranging between 12% and 36%. The relative humidity patterns of the three other cities were remarkably similar, ranging from 22% to 30%. Kuala Lumpur had the highest humidity from April to October, excluding Phnom Penh (Figure 9).

Unlike air temperature, the differences in relative humidity between the office zones and their respective cavity zones of DSF of each location were not as significant throughout the year, only ranging from 1% to 5%. Interestingly, the percentages in the office zones were always higher than in the cavity zones throughout the year, except for Nha Trang, where there were fluctuations. On the other hand, humidities in the north zone were constantly higher than in its respective office zone (Figure 9).

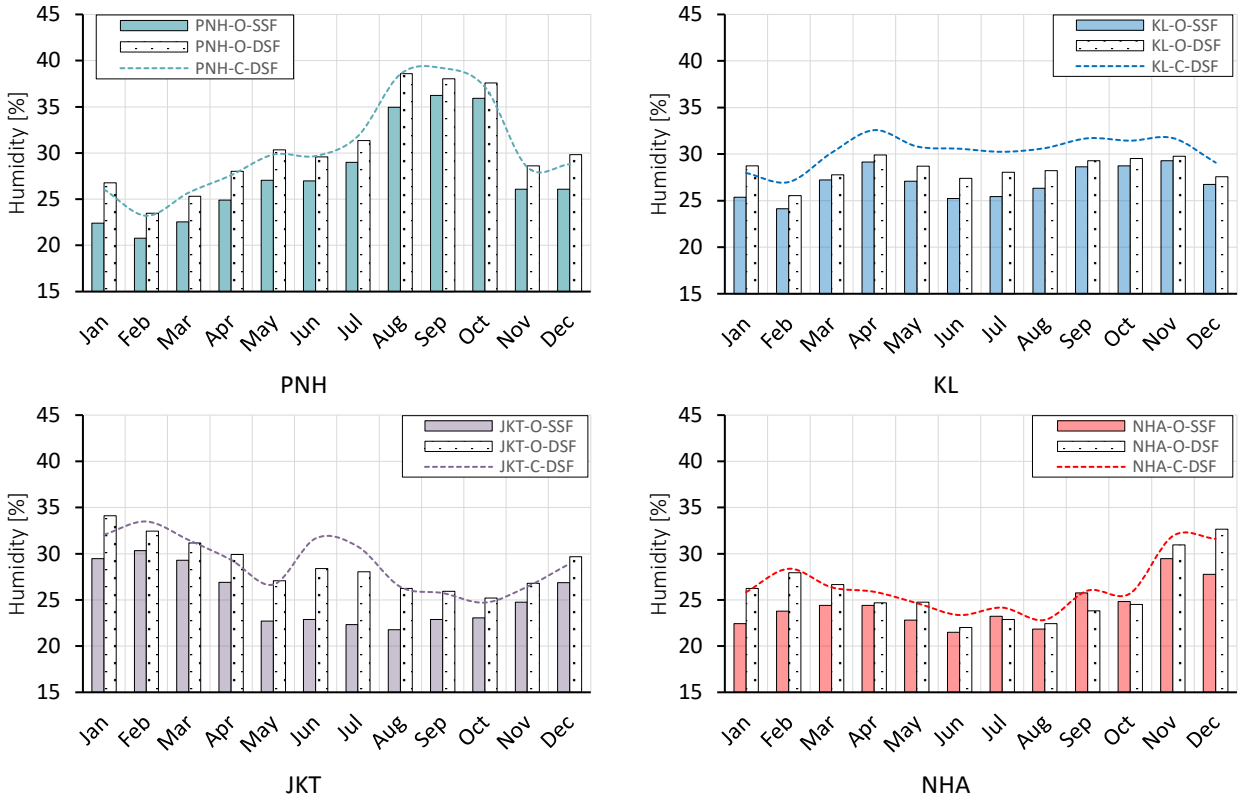

Fig. 9. Monthly average relative humidity in the thermal zones of SSF and DSF of each city

Overall, the relative humidity of the DSF office zones was always higher than the SSF office zones throughout the year. In contrast with air temperature behavior, the DSF office zone was always lower than the SSF zone annually. The percentage of relative humidity in the DSF office zone was usually lower than the SSF office zone by around 3%. However, if we compare it in the DSF office zone and the DSF cavity, it was not the same case that behaved in the opposite way air temperature did; the relative humidity of the DSF cavity could be higher or lower than its office zone unstably throughout the twelve months. In Phnom Penh city, the cavity of the DSF was more humid than its office zone in March, June, and September by around 1%. In Kuala Lumpur, with the most exceptional case among all the cities, humidity in the cavity was typically higher than in its office zone throughout the year, except for January, when it fell behind its office zone by more than 2%. Whereas the cavity zone in Jakarta was more humid in February, March, and from May to August by around 1% to 4% compared to its thermal office zone, while the percentages of relative humidity of the cavity in Nha Trang were higher in February and from June to November around 1% to 4%. These variations may also be affected by the climatic condition of each city and the thermal stack chimney of each cavity zone of the DSF (Figure 10).

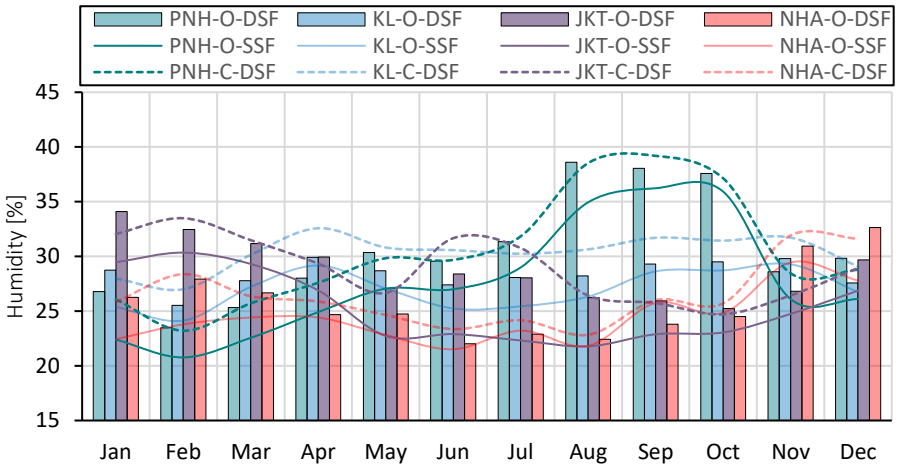

Fig. 10. Comparison of monthly average relative humidity in the thermal zones of SSF and DSF of each city

When looking at the orientations of all thermal zones, the annual average relative humidities in the east thermal office zones of the SSF system of all climate categories were the lowest of all orientations, with an average of 23.4%, while Kuala Lumpur's was the lowest. Interestingly, the highest annual average humidity was in the west thermal office zone of Kuala Lumpur, with 29.4%, followed by Phnom Penh's north office zone, Jakarta's south office zone, and Nha Trang's north office zone, with 29.1%, 27.4 %, and 26.6% respectively (Figure 11).

For both office and cavity zones of the DSF, the annual relative humidity of the east zones was always lower than the zone of other orientations, while Phnom Penh had the highest among other cities by about 3%. It was interesting that the humidities of the north office zones of all classifications were either lower or higher than those of office zones on their own, but its cavity zone was constantly higher by a significant amount by around 4%. It is noticeable that the DSF in Phnom Penh had the highest humidity rate, while Nha Trang had the lowest, and the humidities of the two others were quite comparable (Figure 11).

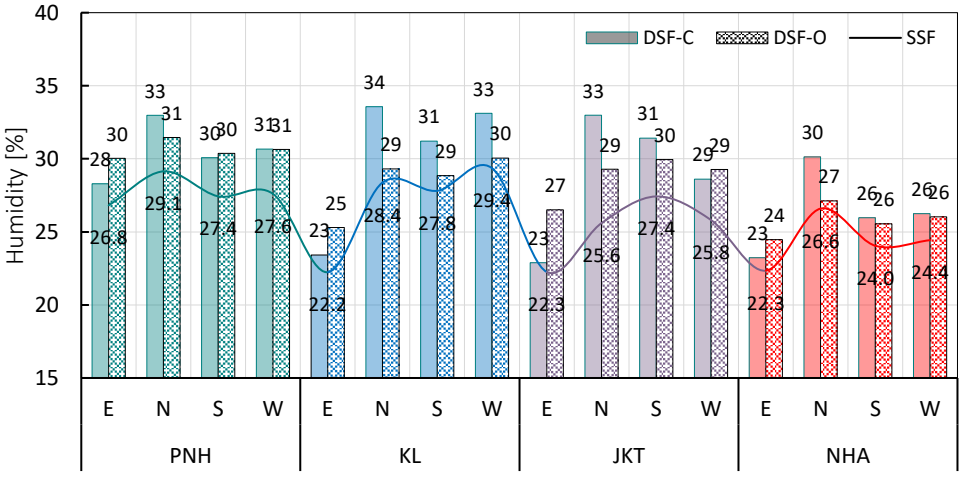

Fig. 11. Comparison of annual average relative humidity in the thermal zones of SSF and DSF-NL at the four orientations of each city

Comparing the two façade systems, the humidity of the DSF office zone increased by around 3% compared with the SSF. The four climate classifications had a spectrum of relative air humidity changes at all orientations but had a typical humidity range of about 3%. The humidity of the DSF

office zone was typically lower than its cavity zone at all facings, apart from the east, which was more humid than its cavity zone in all climate classifications. This phenomenon could also be explained by the behavior of the respective climate and the influence of the air temperature, which appeared to be the highest throughout the year and may have a significant impact on the chimney effect in the cavity of the DSF, increasing the temperature along with a higher annual solar radiation rate. It was also noticeable that the relative humidity of the DSF office and zone and cavity zone were all higher than the SSF office zone at all orientations and all classifications, which were apart from the air temperature case that somehow the cavity zone was hotter than the office zone of the SSF, as shown in Figure 11.

4.3 Zone Window Transmitted Solar Radiation

Before the analysis, it is worth mentioning that these comparisons were between the SSF office zones, which had internal shading, and the DSF cavity zones, which did not have a shading device. As a result, the solar radiations of the DSF cavity zone were significantly higher than those of the SSF office zones. After integrating the second layer into the SSF, the data on solar radiation rate could no longer be obtainable from the simulation.

In the SSF system, solar radiation rates in the thermal office zones of all climate contexts varied from month to month. The solar radiation rate in Phnom Penh city from January to March was comparable with other cities; however, it gradually decreased, reaching the lowest point of all in October, with 300W. Throughout the year, the solar rate in Kuala Lumpur was nearly constant, ranging from around 450W to 550W. Jakarta's solar radiation rate was low in February at around 500W and peaking in September at around 630W, which was the highest of all. Nha Trang had the smallest solar radiation from November to December and the highest in April, with maximum values reaching 620W (Figure 12).

Since the DSF category was not equipped with solar shading, solar radiation rates were so high, reaching the highest point of more than 6000W in the thermal cavity zone of Jakarta, while the lowest solar radiation was achieved by Phnom Penh's cavity zone in October, with only around 3100W. Nevertheless, the solar radiation rates of all cities average, ranging from 3500W to 5500W, with fluctuations throughout the year (Figure 12).

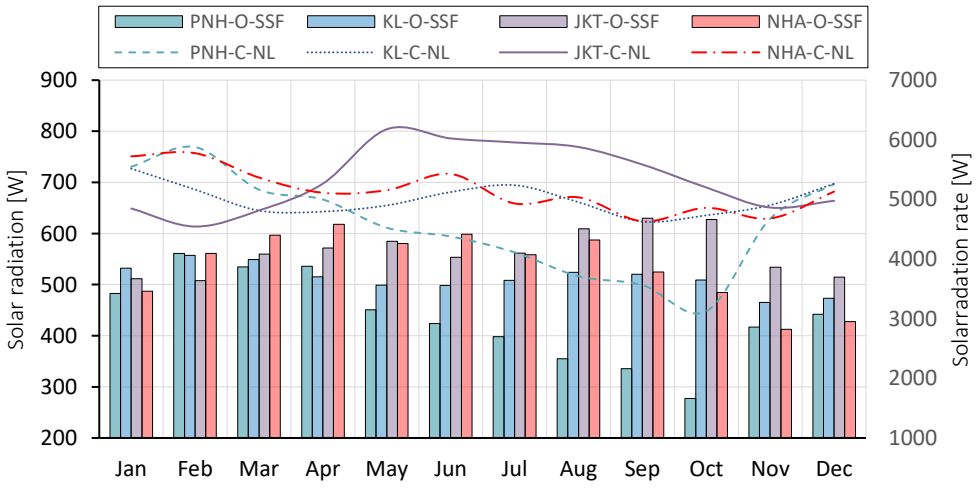

Fig. 12. Comparison of monthly average solar radiation in the thermal zones of SSF office and DSF cavity of each city

However, these comparisons indicated the significant influence of the second skin of the DSF on the thermal performance of the SSF. From monthly indications of all locations, the patterns of solar radiation rate in the DSF cavity zone were not so parallel with the SSF office zone. The ratios of solar radiation between the two categories were quite noticeable, especially in Nha Trang, whose solar radiation patterns were invisibly opposite (Figure 12).

Thermal zones of the SSF of the four cities had the highest annual solar radiation rate in the east, with Jakarta having the highest, with 609W of radiation. On the other hand, the north thermal zones of all cities had the lowest solar radiation rate, except for Jakarta, where the lowest radiation rate was in the south. Phnom Penh, Kuala Lumpur and Nha Trang seemed to have similar attributes, having the highest radiation in the east, followed by the west, the south and the north. Slightly apart from other cities, the smallest amount of radiation was in the south thermal office zone (Figure 13).

Whereas in DSF, all locations and orientations had annual average solar radiations ranging from 3400W to 8500W, with Nha Trang having the lowest in the north and Kuala Lumpur having the highest in the east. The east cavity zones of all climatic categories had the most solar radiation among other orientations of their classification and were followed by the west, the south and the north, respectively, except for Jakarta, the zones with high solar radiation after the east cavity zone were the west, north, and south, in that order. The east cavity zones of Kuala Lumpur had the highest rate, with around 8400 W, followed by Jakarta and Nha Trang. Despite the number of radiation differences, the four orientations of all locations performed comparably (Figure 13).

Overall, the solar radiation rates in the SSF office zones, which had internal shading, were quite similar at all orientations and classifications. However, without the shading device in the DSF cavity zones, the solar radiation rates were altered from face to face, with the east having the highest solar radiation rate, followed by the west, in all classifications. These variations impacted the temperature and humidity changes in the cavity and office zones (Figure 13). According to the previous analyses, the air temperatures were higher in the east of all categories and were comparable to the amount of the solar radiation rates. Without a shading device, the DSF has potentially enhanced the thermal performance of the optimum SSF model, lowering the air temperature and increasing the relative humidity of the office zones.

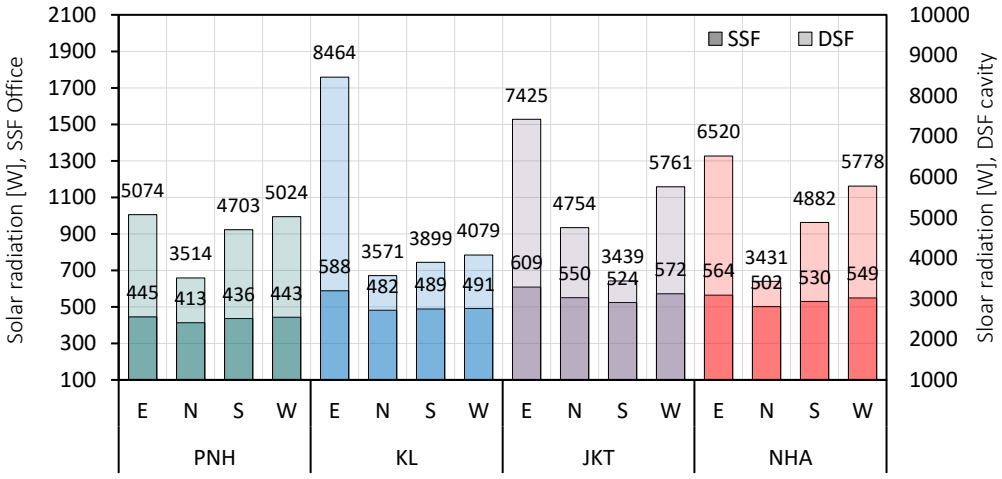

Fig. 13. Comparison of annual average solar radiation in the thermal zones of SSF office and DSF-NL cavity at the four orientations of each city

4.4 Comparison of the Three Environmental Parameters

From the result above, the thermal performances of facades in four classifications were different from month to month and from orientation to orientation. The relation of the three environmental parameters is shown in Figure 14. The profiles of air temperature and solar radiation were quite comparable and worked in contrast with the relative humidity. When air temperatures in the thermal zone were high, the amounts of solar radiation were also high, while humidities turned out to be low.

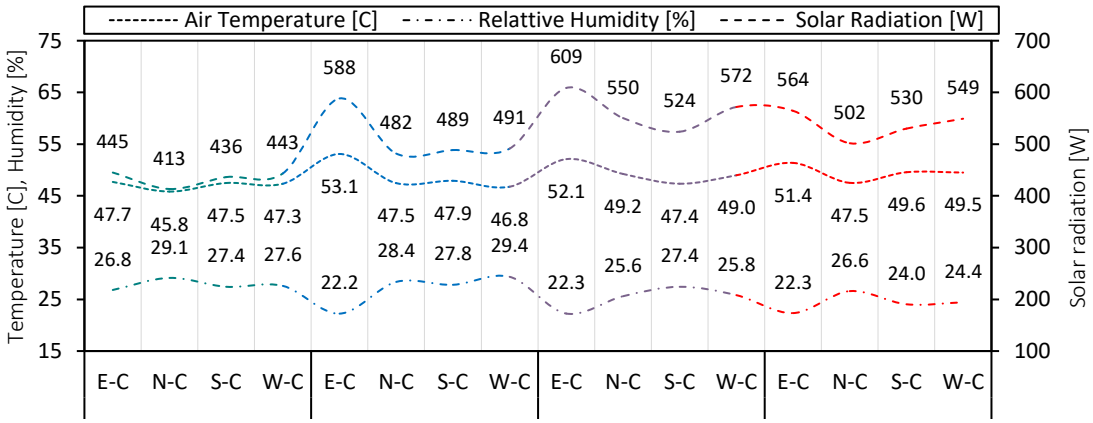

Fig. 14. Thermal behaviors in the thermal zones of SSF at the four orientations of each city

These three parameters might be well correlated, but they might not be completely dependent on one another in terms of thermal changes. Phnom Penh city was one good example of how lower solar radiation had less of an influence on the temperature; even though solar radiations of three other cities were significantly higher than in Phnom Penh, the temperatures of all cities were still comparable, with the numbers of differences were in similar averages ranging from 45°C to 53°C for air temperature, from 22% to 30% for relative air humidity and 400W to 600W for solar radiation rate. From the results above, the thermal and energy performances of SSF were influenced by respective climate classifications (Figure 14).

4.5 Energy Consumption

The different thermal performances of the SSF in different climatic classifications caused the different proportions of energy consumption. The SSF in Jakarta consumed the most for cooling among the four cities, which might be because Jakarta had the highest peak air temperature and solar radiation rate. On the other hand, the fluctuation of air temperature and relative humidity in each city's thermal zones might be the considerable factors influencing energy consumption for cooling. Nonetheless, the energy consumption gaps between the four cities were relatively small, with only around 146MWh (Figure 15).

Similarly, the different thermal performances of the DSF in all cities caused various breakdowns of energy. DSF in Phnom Penh consumed the most for cooling despite having the lowest temperature; annual relative humidity and solar radiation rate might be the reasons for this phenomenon. The instability of air temperature, relative humidity, and solar radiation in each city's thermal zones significantly impacted DSF performances. Even though the four climatic classifications affected the thermal performances of DSF differently, the disparities in energy consumption of the four cities were relatively small, with around an annual mean of 34MWh only (Figure 15).

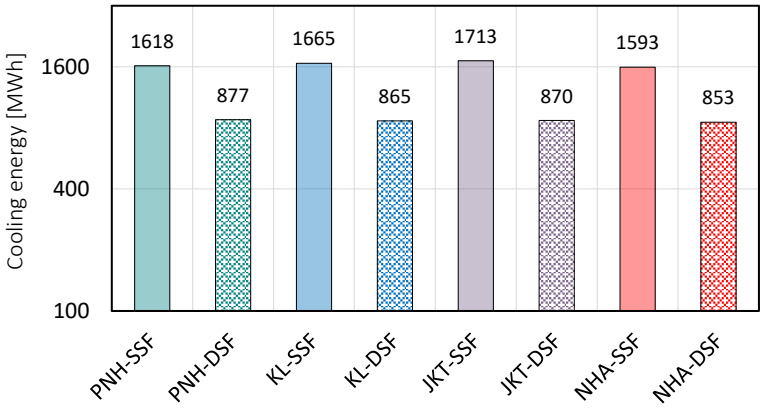

Fig. 15. Comparison of annual energy consumption for cooling of the SSF and the DSF of each city

Comparing the energy consumption of both façade systems, the DSF model consumed less energy than the SFF model of all classifications, with an annual reduction of up to more than 40%. From the SSF categories, the SSF in Jakarta consumed the most energy, followed by those in Kuala Lumpur and Phnom Penh. However, with DSF, Phnom Penh had the highest consumption, even though consumption dropped by about 50%, followed by Jakarta and Kuala Lumpur. This phenomenon may be explained by the climatic conditions of each city, as shown in the preceding sections. For instance, although Jakarta's climate may be the hottest among all categories in the SSF investigations, the consumption differences between the four cities were still negligible (Figure 15). DSF in Phnom Penh, on the other hand, had the most energy consumption, which may be influenced by the environmental conditions and the thermal stack effect, causing the temperature and humidity fluctuation gap in the cavity to be relatively large among all climate classifications.

From the results above, it is comprehensible that the DSF system had a significant impact on the thermal performance of the SSF that hypothetically influenced its energy efficiency. DSF could save energy for air-conditioning up to more than 40%, with air temperature reductions, relative humidity modifications, and thermal chimney effect in the cavity. DSF could be beneficially employed in an overall tropical climate even though the four climate categories classified by Köppen were all considerably distinct throughout the year.

5. Discussion

The discussion started with the SSF category, which will be the base indication of how the DSF could enhance this conventional façade system. The performances of SSF in each tropical category were first analyzed and then benchmarked with the DSF following the findings from previous studies, having been done in similar climatic contexts.

5.1 Performance of the SSF in Tropical Climate

The primary results agreed with most previous studies that particular locations and climates might affect thermal performance in a building differently. The SSF in the four selected cities, which were in the tropical classes, exhibited diverse thermal behaviors throughout the year. The two main thermal variables chosen for investigation behaved differently in the SSF thermal zone; air temperature and relative humidity behaved differently in respective climates. It tended to vary from month to month and from orientation to orientation. It is noteworthy that when the air temperature

in the thermal zone was high, the relative humidity was low. This phenomenon occurred in all cases and influenced the overall energy performance of buildings in all cities.

Although SSF in the four tropical categories behaved inversely, the range of air temperature and relative humidity in the SSF thermal zone in all cities was not that different, ranging from 40^{o}C to 53^{o}C and 20% to 36%, respectively. As a result, there was no significant difference in annual thermal and energy performance across all tropical categories. Furthermore, the difference in average annual energy consumption for cooling in SSF across all cities was only about 5%.

5.2 Performance of the DSF in Tropical Climate

This section discusses the findings that compared the thermal and energy performance of DSF to SSF in an overall tropical climate. The thermal and energy performances of the DSF are influenced by climatic conditions, classifications and technical aspects. Therefore, the proposed DSF modeling followed the most efficient classifications and technical aspects recommended in the previous studies having been done in similar weather contexts. For instance, Hong *et al.,* [6] claimed that multi-story DSF with natural ventilation could reduce cooling energy by up to 12% in the monsoon climate. Additionally, incorporating a naturally ventilated cavity on all orientations of the building in tropical rainforest climate would decrease the cooling load over conventional single-skin façades by up to more than 46%, as stated by Ayegbusi *et al.,* [58]. Saroglou *et al.,* [59] demonstrated that naturally ventilated DSF in hot and Mediterranean climates could save up to 50% of energy when combined with one-meter to two-meter cavity depth and low-e glazing on the interior and exterior layers of the façade. Also, Alberto *et al.,* [60] found that a multi-story DSF with a one-meter cavity depth was the most efficient in a mild climate. He continued by claiming that the significant aspect of DSF was the airflow path. Parra *et al.,* [61] discovered that the technical aspects strongly influenced the air temperature and airflow behaviors of naturally ventilated DSF. Other studies also came to similar conclusions about the classification and technical aspects of DSF that provide better performance in the same tropical climate context.

From the results obtained, they were predominantly agreeable with all the above findings. However, the outcomes might differ in terms of efficiency. In line with the prediction, DSF in all tropical groups could significantly improve thermal performance in SSF. The air temperature in the SFF thermal office zone was reduced by about 4^{o}C, while relative humidity increased by about 1% to 5%. These thermal parameters fluctuated throughout the year but consistently ranged from 40^{o}C to 52^{o}C and 21% to 39%, respectively. Due to this similarity, the energy performance of DSF was also marginally performed in all tropical classes. The difference in average annual energy consumption variation was only 4%. Therefore, DSF could be beneficial for glass buildings in tropical climates, having the capacity to enhance and improve thermal and energy performance.

6. Conclusion

The primary conclusion for this investigation is that the SSF of the different tropical classified groups had diverse thermal behaviors over the entire year. From month to month and from orientation to orientation, the indoor environment of the SSF office zone varied correspondingly to its individual climatic conditions. However, air temperature and relative humidity in the SSF zone remained in a predictable range throughout the year, ranging from 40^{o}C to 53^{o}C and 20% to 36%, respectively. As a result of this similarity, the cooling energy consumptions of the SSF in the four cities were distinctly comparable, with the gap in energy consumption being around 5%. Therefore,

thermal behaviors and energy intake of the SSF varied dramatically on a monthly basis but only slightly on an annual basis.

After the analysis of DSF in the individual city, it was found that DSF certainly was influenced by the respective climate of each tropical group. Without any shading device, the solar radiation rate in the cavity zone of DSF was high compared to the SSF office zone. Even so, DSF still had the potential to reduce cooling energy to more than 40% in all climatic contexts. The air temperature of the office zone was decreased to around 4^{o}C, while relative humidity increased from 1% to 5%. Following these enhancements, energy consumption for air conditioning in all cities dropped by about 40%. DSF could improve the building's thermal performance and energy efficiency in the Köppen tropical classified climate.

The findings of this study provided a deep knowledge of DSF in the context of a tropical climate, implying that this façade system might be an environmentally friendly façade with optimal configurations to improve the indoor environment of a high-rise glass building. This research has given further DSF knowledge to designers and/or engineers regarding the proper application of DSF to achieve optimal performance in high-rise glass façades, particularly in tropical climates.

Acknowledgment
This research was partially supported by the Documentation Center of Cambodia (DC-Cam).

References

[1] Barbosa, Sabrina, and Kenneth Ip. "The impact of double skin facade on the energy consumption of office buildings under the tropical Brazilian climate." In *World Sustainable Built Environment Conference*, pp. 284-289. 2017.
[2] Loncour, Xavier, Arnaud Deneyer, Marcelo Blasco, G. Flamant, and P. Wouters. "Ventilated double facades. Classification & illustration of façade concepts." *Belgian Building Research Institute* 8 (2004): 15-17.
[3] Hendriksen, Ole J., H. Sorensen, A. Svenson, and Pontus Aaqvist. "Double Skin Façades-Fashion or a step towards sustainable buildings." *Proceedings of ISES, Eurosun* 2000 (2000).
[4] Streicher, Wolfgang, Richard Heimrath, Herwig Hengsberger, Thomas Mach, Reinhard Waldner, Gilles Flamant, Xavier Loncour et al. "On the typology, costs, energy performance, environmental quality and operational characteristics of double skin façades in european buildings." *Advances in Building Energy Research* 1, no. 1 (2007): 1-28. https://doi.org/10.1080/17512549.2007.9687267
[5] Waldner, R., G. F. S. Prieus, H. Erhorn-Kluttig, I. Farou, R. Duarte, C. Blomqvist, N. Kiossefidi, D. Geysels, G. Guarracino, and B. Moujalled. "BESTFACADE, Best Practice for Double Skin Façades, WP5 Best Practice Guidelines." *Energy and Building Design, EIE/04/135 S 7* (2007).
[6] Hong, Taehoon, Jimin Kim, Juyoung Lee, Choongwan Koo, and Hyo Seon Park. "Assessment of seasonal energy efficiency strategies of a double skin façade in a monsoon climate region." *Energies* 6, no. 9 (2013): 4352-4376. https://doi.org/10.3390/en6094352
[7] Poirazis, Harris. *Double skin façades for office buildings*. Report EBD, 2004.
[8] Pollard, Brett. "DOUBLE SKIN FAÇADES-MORE IS LESS?." *Environment Design Guide* (2009): 1-10.
[9] Faggal, Ahmed Atef. "Double Skin Façade Effect on Thermal Comfort and Energy Consumption in Office Buildings." *Ain Shams University*, 2006.
[10] Aksamija, Ajla. "Energy Performance Of Different Types Of Double Skin Facades In Various Climates." *Department of Architecture* (2016).
[11] Cooper, Dean. "Energy Efficiency for Buildings." *UNEP*, 2022.
[12] Katili, Adrian R., Rabah Boukhanouf, and Robin Wilson. "Space cooling in buildings in hot and humid climates-a review of the effect of humidity on the applicability of existing cooling techniques." In *14th International Conference on Sustainable Energy Technologies - SET 2015*. 2015.
[13] Inan, Tugba, and Tahsin Basaran. "Experimental and numerical investigation of forced convection in a double skin façade by using nodal network approach for Istanbul." *Solar Energy* 183 (2019): 441-452. https://doi.org/10.1016/j.solener.2019.03.030
[14] Azarbayjani, Mona. "Comparative performance evaluation of a multistory double skin façade building in humid continental climate." In *ARCC Conference Repository*. 2013.
[15] Rahmani, Behzad, Mohd Zin Kandar, and Parisa Rahmani. "How double skin façade's air-gap sizes effect on lowering solar heat gain in tropical climate?." *World Applied Sciences Journal* 18, no. 6 (2012): 774-778.

[16] Qahtan, Abdultawab M. "Thermal performance of a double-skin façade exposed to direct solar radiation in the tropical climate of Malaysia: A case study." *Case Studies in Thermal Engineering* 14 (2019): 100419. https://doi.org/10.1016/j.csite.2019.100419
[17] Arons, Daniel M. M. "Properties and applications of double-skin building facades." *PhD diss., Massachusetts Institute of Technology*, 2000.
[18] Boake, Terri M., Kate Harrison, David Collins, Taymoore Balbaa, Andrew Chatham, Richard Lee, and Andre Bohren. "The tectonics of the double skin." In *Proc., ARCC Conf. Repository. San Antonio: Architectural Research Centers Consortium*. 2002.
[19] Chan, A. L. S., Tin Tai Chow, K. F. Fong, and Z. Lin. "Investigation on energy performance of double skin façade in Hong Kong." *Energy and Buildings* 41, no. 11 (2009): 1135-1142. https://doi.org/10.1016/j.enbuild.2009.05.012
[20] Saelens, Dirk, Jan Carmeliet, and Hugo Hens. "Energy performance assessment of multiple-skin facades." *HVAC&R Research* 9, no. 2 (2003): 167-185. https://doi.org/10.1080/10789669.2003.10391063
[21] Ghaffarianhoseini, Ali, Amirhosein Ghaffarianhoseini, Umberto Berardi, John Tookey, Danny Hin Wa Li, and Shahab Kariminia. "Exploring the advantages and challenges of double-skin façades (DSFs)." *Renewable and Sustainable Energy Reviews* 60 (2016): 1052-1065. https://doi.org/10.1016/j.rser.2016.01.130
[22] Tao, Yao, Haihua Zhang, Lili Zhang, Guomin Zhang, Jiyuan Tu, and Long Shi. "Ventilation performance of a naturally ventilated double-skin façade in buildings." *Renewable Energy* 167 (2021): 184-198. https://doi.org/10.1016/j.renene.2020.11.073
[23] Kim, Daeung Danny. "Computational fluid dynamics assessment for the thermal performance of double-skin façades in office buildings under hot climatic condition." *Building Services Engineering Research and Technology* 42, no. 1 (2021): 45-61. https://doi.org/10.1177/0143624420952962
[24] Regazzoli, A. "A Comparative Analysis On The Effect Of Double-Skin Façade Typologies On Overall Building Energy Consumption Performance In A Temperate Climate." *Undergraduate. Dublin Institute of Technology* (2013).
[25] Aksamija, Ajla. "Context Based Design of Double Skin Facades." *Perkins+ Will Research Journal* 1, no. 1 (2009): 54-69.
[26] Tao, Yao, Haihua Zhang, Dongmei Huang, Chuangang Fan, Jiyuan Tu, and Long Shi. "Ventilation performance of a naturally ventilated double skin façade with low-e glazing." *Energy* 229 (2021): 120706. https://doi.org/10.1016/j.energy.2021.120706
[27] Haase, M., and A. Amato. "Design considerations for double-skin facades in hot and humid climates." *Envelope Technologies for Building Energy Efficiency* 2 (2006).
[28] Lim, Yonghuort, and Mohd Rodzi Ismail. "Efficacy of Double Skin Façade on Energy Consumption in Office Buildings in Phnom Penh City." *International Transaction Journal of Engineering, Management, & Applied Sciences & Technologies* 9, no. 2 (2018): 119-132.
[29] Kim, Dongsu, Sam J. Cox, Heejin Cho, and Jongho Yoon. "Comparative investigation on building energy performance of double skin façade (DSF) with interior or exterior slat blinds." *Journal of Building Engineering* 20 (2018): 411-423. https://doi.org/10.1016/j.jobe.2018.08.012
[30] Lee, Jeehwan, Mohammed Alshayeb, and Jae D. Chang. "A study of shading device configuration on the natural ventilation efficiency and energy performance of a double skin façade." *Procedia Engineering* 118 (2015): 310-317. https://doi.org/10.1016/j.proeng.2015.08.432
[31] Balocco, Carla. "A non-dimensional analysis of a ventilated double façade energy performance." *Energy and Buildings* 36, no. 1 (2004): 35-40. https://doi.org/10.1016/S0378-7788(03)00086-0
[32] Baldinelli, Giorgio. "Double skin façades for warm climate regions: Analysis of a solution with an integrated movable shading system." *Building and Environment* 44, no. 6 (2009): 1107-1118. https://doi.org/10.1016/j.buildenv.2008.08.005
[33] Haase, Matthias, and Alex Amato. "A study of the effectiveness of different control strategies in double skin facades in warm and humid climates." *Journal of Building Performance Simulation* 2, no. 3 (2009): 179-187. https://doi.org/10.1080/19401490902984929
[34] Gavan, Valentin, Monika Woloszyn, Jean-Jacques Roux, Cristian Muresan, and Nassim Safer. "An investigation into the effect of ventilated double-skin facade with venetian blinds: Global simulation and assessment of energy performance." *Proceedings: Building Simulation* (2007).
[35] Oesterle, Eberhard. *Double-skin facades: integrated planning, building physics, construction, aerophysics, air-conditioning, economic viability*. Prestel: Munich, 2001.
[36] Tascón, Mauricio Hernandez. "Experimental and computational evaluation of thermal performance and overheating in double skin facades." *PhD diss., University of Nottingham*, 2008.
[37] Fu, Tat S., and Rui Zhang. "Integrating double-skin façades and mass dampers for structural safety and energy efficiency." *Journal of Architectural Engineering* 22, no. 4 (2016): 04016014. https://doi.org/10.1061/(ASCE)AE.1943-5568.0000218

[38] Souza, Eduardo. "How do double-skin façades work?." *ArchDaily*. August 20, 2019. https://www.archdaily.com/922897/how-do-double-skin-facades-work.
[39] Su, Ziyi, Xiaofeng Li, and Fei Xue. "Double-skin façade optimization design for different climate zones in China." *Solar Energy* 155 (2017): 281-290. https://doi.org/10.1016/j.solener.2017.06.042
[40] Li, Yilin, Jo Darkwa, Georgios Kokogiannakis, and Weiguang Su. "Phase change material blind system for double skin façade integration: System development and thermal performance evaluation." *Applied Energy* 252 (2019): 113376. https://doi.org/10.1016/j.apenergy.2019.113376
[41] Bayram, Ayça. "Energy performance of duble-skin fąacades in intelligent office buildings: a case study in Germany." *Master's thesis, Middle East Technical University*, 2003.
[42] Zhu, Yimin. "Applying computer-based simulation to energy auditing: A case study." *Energy and Buildings* 38, no. 5 (2006): 421-428. https://doi.org/10.1016/j.enbuild.2005.07.007
[43] Chowdhury, Ashfaque Ahmed, M. G. Rasul, and M. M. K. Khan. "Modelling and simulation of building energy consumption: a case study on an institutional building in central Queensland, Australia." *Proceedings: Building Simulation* (2007): 1916-1923.
[44] Canyurt, Olcay Ersel, Harun Kemal Ozturk, Arif Hepbasli, and Zafer Utlu. "Estimating the Turkish residential-commercial energy output based on genetic algorithm (GA) approaches." *Energy Policy* 33, no. 8 (2005): 1011-1019. https://doi.org/10.1016/j.enpol.2003.11.001
[45] Köppen, W. "Classification of climates according to temperature, precipitation and seasonal cycle." *Petermanns Geographische Mitteilungen* 64, no. 1918 (1918): 193-203.
[46] Stadler, Michael, Ryan Firestone, Dimitri Curtil, and Chris Marnay. *On-site generation simulation with energyplus for commercial buildings*. No. LBNL-60204. Lawrence Berkeley National Lab.(LBNL), Berkeley, CA (United States), 2006.
[47] U.S. Deparment of Energy. " EnergyPlus™ Version 22.2.0 Documentation - Getting Started." *EnergyPlus*, 2022. https://energyplus.net/assets/nrel_custom/pdfs/pdfs_v22.2.0/GettingStarted.pdf.
[48] Joe, Jaewan, Wonjun Choi, Younghoon Kwak, and Jung-Ho Huh. "Optimal design of a multi-story double skin facade." *Energy and Buildings* 76 (2014): 143-150. https://doi.org/10.1016/j.enbuild.2014.03.002
[49] Anđelković, Aleksandar S., Igor Mujan, and Stojanka Dakić. "Experimental validation of a EnergyPlus model: Application of a multi-storey naturally ventilated double skin façade." *Energy and Buildings* 118 (2016): 27-36. https://doi.org/10.1016/j.enbuild.2016.02.045
[50] Im, Piljae, Joshua Ryan New, and Jaewan Joe. *Empirical validation of building energy modeling using flexible research platform*. Oak Ridge National Lab.(ORNL), Oak Ridge, TN (United States), 2019.
[51] Lucchino, Elena Catto, Adrienn Gelesz, Kristian Skeie, Giovanni Gennaro, András Reith, Valentina Serra, and Francesco Goia. "Modelling double skin façades (DSFs) in whole-building energy simulation tools: Validation and inter-software comparison of a mechanically ventilated single-story DSF." *Building and Environment* 199 (2021): 107906. https://doi.org/10.1016/j.buildenv.2021.107906
[52] Fallahi, Ali, Fariborz Haghighat, and Hafia Elsadi. "Energy performance assessment of double-skin façade with thermal mass." *Energy and Buildings* 42, no. 9 (2010): 1499-1509. https://doi.org/10.1016/j.enbuild.2010.03.020
[53] Tabares-Velasco, Paulo Cesar, Craig Christensen, and Marcus Bianchi. "Verification and validation of EnergyPlus phase change material model for opaque wall assemblies." *Building and Environment* 54 (2012): 186-196. https://doi.org/10.1016/j.buildenv.2012.02.019
[54] Pereira, Welma, Andreas Bögl, and Thomas Natschläger. "Sensitivity analysis and validation of an EnergyPlus model of a house in Upper Austria." *Energy Procedia* 62 (2014): 472-481. https://doi.org/10.1016/j.egypro.2014.12.409
[55] Mateus, Nuno M., Armando Pinto, and Guilherme Carrilho Da Graça. "Validation of EnergyPlus thermal simulation of a double skin naturally and mechanically ventilated test cell." *Energy and Buildings* 75 (2014): 511-522. https://doi.org/10.1016/j.enbuild.2014.02.043
[56] Beck, Hylke E., Niklaus E. Zimmermann, Tim R. McVicar, Noemi Vergopolan, Alexis Berg, and Eric F. Wood. "Present and future Köppen-Geiger climate classification maps at 1-km resolution." *Scientific Data* 5, no. 1 (2018): 1-12. https://doi.org/10.1038/sdata.2018.214
[57] Lim, Yonghuort, and Mohd Rodzi Ismail. "Aptitudes of Double Skin Façade Toward Green Building within Built Environment." *Journal of Advanced Research in Fluid Mechanics and Thermal Sciences* 100, no. 3 (2022): 146-170. https://doi.org/10.37934/arfmts.100.3.146170
[58] Ayegbusi, Olutobi Gbenga, Abdullah Sani Ahmad, and Yaik Wah Lim. "Overall Thermal Transfer Value of Naturally Ventilated Double Skin Façade in Malaysia." *Progress in Energy and Environment* 5 (2018): 16-26.
[59] Saroglou, Tanya, Theodoros Theodosiou, Baruch Givoni, and Isaac A. Meir. "Studies on the optimum double-skin curtain wall design for high-rise buildings in the Mediterranean climate." *Energy and Buildings* 208 (2020): 109641. https://doi.org/10.1016/j.enbuild.2019.109641

[60] Alberto, André, Nuno MM Ramos, and Ricardo MSF Almeida. "Parametric study of double-skin facades performance in mild climate countries." *Journal of Building Engineering* 12 (2017): 87-98. https://doi.org/10.1016/j.jobe.2017.05.013

[61] Parra, Jordi, Alfredo Guardo, Eduard Egusquiza, and Pere Alavedra. "Thermal performance of ventilated double skin façades with venetian blinds." *Energies* 8, no. 6 (2015): 4882-4898. https://doi.org/10.3390/en8064882